

Substrate Metabolism and Mitochondrial Function in Skeletal Muscle of Amyloid Precursor Protein-Overexpressing Mice

Elika Shabrokh¹,
John Kavanaugh²,
Ryan McMillan^{2,3},
Yaru Wu², Matt Hulver^{2,3} and
Madlyn Frisard^{2,3}

Abstract

Background: Sporadic Inclusion body myositis (sIBM) is an idiopathic inflammatory myopathy that involves inflammation and damage to skeletal muscle tissue. Studies in humans demonstrate altered mitochondrial morphology in skeletal muscle from patients diagnosed with sIBM suggesting mitochondrial defects may be a significant contributor to disease progression.

Methods: MCK-APP mice, overexpress amyloid precursor protein specifically in skeletal muscle, display characteristics of sIBM, and are an accepted model to study disease pathology.

Results: The current studies demonstrate a significant reduction in fat oxidation and oxidative efficiency in white gastrocnemius muscle in 9-month-old MCK-APP. However, there were no differences in mitochondrial bioenergetics or the production of reactive oxygen species in red or white gastrocnemius muscle in 3, 6, or 9-month-old MCK-APP mice compared to wild-type littermates.

Conclusion: Functional alterations in mitochondria are not yet pronounced in 3, 6, and 9-month-old MCK-APP mice prior to symptom development; however alterations in substrate metabolism in white skeletal muscle may be present.

Keywords: Amyloid precursor protein, Amyloid beta, Bioenergetics, Fatty acid oxidation, Mitochondrial metabolism, Skeletal muscle metabolism, Reactive oxygen species

- 1 Department of Surgery, University of Michigan Medical School, USA
- 2 Department of Human Nutrition, Foods, and Exercise, Virginia Tech, Blacksburg, USA
- 3 The Metabolic Phenotyping Core at Virginia Tech, Blacksburg, VA, USA

Corresponding author: Madlyn Frisard

✉ frisardm@vt.edu

Department of Human Nutrition, Foods and Exercise. 1981 Kraft Drive, 1085 ILSB, Blacksburg, Virginia 24060, USA

Tel: 540-231-9994

Fax: 540-231-5522

Citation: Shabrokh E, Kavanaugh J, McMillan R et al. Effect of the Addition of Hand-Mixed Generic Vancomycin on Bone Cement Strength. *Ann Clin Lab Res.* 2015, 3:4.

Received: August 28, 2015, **Accepted:** December 15, 2015, **Published:** December 22, 2015

Introduction

Sporadic Inclusion Body Myositis (sIBM) is an inflammatory muscle disease that strikes individuals at random and accounts for approximately 1/3 of all idiopathic inflammatory myopathies [1]. The disease is characterized by progressive weakness and wasting of the proximal and distal muscles ultimately resulting in restricted movement and mobility [2]. Individuals afflicted with the disorder may be restricted from performing activities of daily living and are often confined to the use of a walking aid or wheelchair [2]. Currently, there is no known cause or cure for sIBM, nor are there any long-term treatment options [3]. Patients do not generally respond to anti-inflammatory, immunosuppressant, or

immune modulatory drugs and treatment of the disease usually includes symptom management and utilizing therapy to maintain mobilization [14,5]. The identification of novel mechanism(s) contributing to disease progression and/or muscle defects may provide new opportunities for prevention and/or treatment of the disorder.

MCK-APP mice, overexpress amyloid precursor protein specifically in skeletal muscle and display characteristics of the disease starting at approximately 10 months of age [6]. MCK-APP mice are considered an accepted model of sIBM and have been used to identify potential mechanism(s) contributing to disease pathology [6]. Recently, mitochondrial impairments such as mitochondrial membrane depolarization and calcium

dysregulation have been observed in 3-month-old MCK-APP mice [7]. Furthermore, glutathione administration to reduce intracellular reactive oxygen species (ROS) concentrations in cells cultured from this model also reduced calcium leak and restored membrane potential implicating the role of intracellular ROS concentrations in mitochondrial dysfunction and disease progression. However, whether mitochondrial dysfunction, specifically mitochondrial bioenergetics, reactive oxygen species production, and dysregulated metabolism occurs in these mice is not yet known [8,9]. The purpose of this study was to examine mitochondrial bioenergetics, substrate metabolism, and production of reactive oxygen species in mitochondria isolated from skeletal muscle from 3, 6, and 9-month old MCK-APP mice.

Material and Methods

Animal model

MCK-APP mice with muscle-specific over-expression of the APP gene were obtained from the original lineage of mice from Dr. Alex Shtifman and used for the experiments proposed in this study [8,10,11]. The transgenic mice (MCK-APP) selectively overexpress human APP and accumulate A β 42 in affected muscle fibers, both of which are important features observed in sIBM patients [12,13]. A recent study has highlighted that overexpression of APP in a new lineage does not lead to the accumulation of amyloid beta nor the development of sIBM like symptoms [14]. The mice used in the current work were from the original lineage and therefore exhibit accumulation of amyloid beta. This animal model also shows motor impairments, which is usually the partial or total loss of function of limbs as a result of muscle weakness, becoming exacerbated in an age-dependent manner [6,10]. Based on previous studies this animal model is an accepted model of sIBM [12,13]. Three, six, and nine month old MCK-APP mice and their wild type littermates were used for the current studies.

Immediately following a 12-hour fast, the animals were sacrificed using carbon dioxide asphyxiation. Skeletal muscle was harvested (gastrocnemius and quadriceps femoris muscle) for measures described below. Red and white skeletal muscle was manually separated based on visual detection. Skeletal muscle homogenate preparations were used for assessment of fatty acid oxidation, pyruvate dehydrogenase activity, metabolic flexibility, and oxidative efficiency. Mitochondria were isolated from skeletal muscle for measures of mitochondrial respiration, fatty acid oxidation, and reactive oxygen species production. Tissue samples were also collected and immediately stored for later analysis of mRNA expression and enzyme activity. All mouse studies were performed under an approved protocol by the Institutional Animal Care and Use Committee at Virginia Tech.

Skeletal muscle whole homogenate preparation

Approximately 50 mg of fresh muscle samples were immediately placed into 0.2 ml of a modified sucrose EDTA medium (SET) on ice containing 250 mM sucrose, 1 mM EDTA, 10 mM tris-HCl, and 1 mM ATP, pH 7.4. Muscle samples were then minced with scissors and SET buffer was added to a 20-fold diluted (wt:vol) suspension. The minced samples were homogenized in a Potter-

Elvehjem glass homogenizer at 10 passes across 30 seconds at 1,200 rpm with a motor-driven teflon pestle, and measures of fatty acid oxidation, and maximal enzyme activities were performed.

Fatty acid oxidation

Fatty acid oxidation was assessed in red and white gastrocnemius and quadriceps femoris muscle by measuring and summing $^{14}\text{CO}_2$ production and ^{14}C -labeled acid-soluble metabolites from the oxidation of [1- ^{14}C]-palmitic acid (Perkin Elmer, Waltham, MA), respectively. Briefly, samples were incubated in 0.5 $\mu\text{Ci/ml}$ of [1- ^{14}C]-palmitic acid for 3 hours. Media was then removed and exposed to 200 μl , of 70% perchloric acid for 1 hour to liberate $^{14}\text{CO}_2$, which was trapped in a tube containing 1 M NaOH. The NaOH was then placed into a scintillation vial with 5 ml scintillation fluid. The vial was then placed on a scintillation counter (LS 4500, Beckman Coulter) and counted for the presence of ^{14}C . Acid soluble metabolites were determined by collecting the acidified media and measuring ^{14}C content.

Pyruvate dehydrogenase activity (PDH), metabolic flexibility and oxidative efficiency

Pyruvate oxidation was used to assess the activity of pyruvate dehydrogenase (PDH), the enzyme that catalyzes the oxidation of pyruvate resulting in the provision of glucose-derived acetyl CoA to the TCA cycle [15,16]. [1- ^{14}C]-pyruvate oxidation was assessed in a similar manner to fatty acid oxidation with the exception that pyruvate was substituted for BSA-bound palmitic acid [17,18].

Metabolic flexibility was assessed by measuring [1- ^{14}C] pyruvate oxidation \pm non-labeled BSA (0.5%) bound-palmitic acid. Flexibility is denoted by the percentage decrease in pyruvate oxidation in the presence of free fatty acid (e.g. a higher percentage is indicative of greater metabolic flexibility). It is expressed as the ratio of CO_2 production with labeled pyruvate over CO_2 production with labeled pyruvate in the presence of palmitate.

Oxidative efficiency was calculated by dividing CO_2 production by acid soluble metabolite (ASMs) production and expressed as a ratio.

Enzyme activity

Maximal enzyme activities were assessed in muscle homogenates prepared in a sample buffer containing modified sucrose EDTA medium (SET) on ice containing 250 mM sucrose, 1 mM EDTA, 10 mM tris-HCl, and 1 mM ATP, pH 7.4. Citrate synthase activity was determined by the rate of DNTB reduction upon exposure to acetyl CoA at 412 nm. β -3-hydroxyacyl coenzyme A dehydrogenase (BHAD) and Malate dehydrogenase (MDH) activity was determined by the rate of NADH oxidation in the presence of acetoacetyl coA or oxaloacetate, respectively (340 nm).

Mitochondrial isolation

Mitochondria were isolated from red and white gastrocnemius and quadriceps femoris muscle as previously described with modifications [19]. Freshly dissected muscle was placed in ice-cold buffer 1 for mitochondrial isolation (IBM1) containing 97

mM of sucrose, 50 mM Tris/HCl, 50 mM KCl, 10 mM EDTA/Tris, and 0.2% BSA. The fat and connective tissue was removed and the muscle was minced into very small pieces (<10 mg). The tissue was transferred to a cell strainer, rinsed with PBS/EDTA, and placed in IBM1/0.05% trypsin for digestion for 30 minutes. The sample was then centrifuged at 200 g for 3 minutes at 4°C, the supernatant removed and the pellet was resuspended in IBM1. The sample was homogenized using a Potter Ehlvehjem glass/teflon homogenizer (Thomas Scientific, Swedesboro, NJ), centrifuged at 700 g for 10 minutes at 4°C. The supernatant was transferred to a polypropylene tube and was centrifuged at 8000 g for 10 minutes at 4°C. The supernatant was carefully removed and the pellet suspended in buffer 2 for mitochondrial isolation (IBM2) containing 250 mM Sucrose, 3 mM EGTA/Tris, 10 mM Tris HCl and then centrifuged again at 8000 g for 10 minutes at 4°C. Finally, the supernatant was carefully discarded and the pellet was resuspended in 200µL of IBM2. Protein concentration was determined using the bicinchoninic acid (BCA) assay (Thermo Scientific, Rockford, IL).

Respiration in isolated mitochondria

Respirometry measures of isolated mitochondria were performed using an XF24 extracellular flux analyzer (Seahorse Bioscience, North Billerica, MA). Following mitochondrial isolation, mitochondria were plated on Seahorse cell culture plates at a concentration of 5 µg/well in the presence of 10 mM pyruvate (P5280; Sigma-Aldrich, St. Louis, MO) and 5 mM malate (P5280; Sigma-Aldrich, St. Louis, MO). Experiments consisted of 25 second mixing and 4-7 minute measurement cycles. Oxygen consumption was measured under basal conditions in the presence of pyruvate and malate (state 2), ADP (5 mM, Sigma-Aldrich, St. Louis, MO) stimulated respiration (State 3), oligomycin (2µM) insensitive respiration (State 4_o), and uncoupled, maximal respiration in the presence of FCCP (0.3 µM) to assess respiratory capacity (State 3_u). Respiratory control ratio (RCR) was calculated as the ratio of ADP stimulated state 3 and oligomycin induced state 4 respiration. Oligomycin induced state 4 respiration was used in this ratio to account for any contaminating ATPase activity that may prevent the restoration of low respiration rates. Data are expressed as pmol/min. All experiments were performed at 37°C.

Reactive oxygen species production

ROS production in isolated mitochondria was assessed using Amplex Red. Amplex® Red reagent is a colorless substrate that reacts with hydrogen peroxide (H₂O₂) with a 1:1 stoichiometry to produce highly fluorescent resorufin (excitation/emission maxima=570/585 nm). H₂O₂ is produced from the conversion of superoxide to H₂O₂ by endogenous superoxide dismutase (SOD) in the matrix [20,21]. To measure ROS production from complex 1, complex 3, and reverse electron transfer (REV), isolated mitochondria were plated on a 96-well black plate at a concentration of 5 µg/well under three different conditions, respectively. The three conditions were pyruvate (20 mM)/malate (10 mM)/oligomycin (2 µM)/rotenone (200 nM) for complex 1, pyruvate (20 mM)/malate (10 mM)/oligomycin (2 µM)/SOD (400 U/ml)/antimycin A (2 µM) for complex 3, and succinate (20 mM)/

oligomycin (2 µM) for reverse electron flow to complex 1 (REV). Experiments were conducted in sucrose/mannitol solution in order to maintain mitochondrial integrity. Experiments consisted of 1-minute delay and 1 minute reading cycles, followed by a 5 second mixing cycle performed every third reading. All experiments were performed at 37°C. Measures for ROS levels were conducted on a microplate reader (Biotek synergy 2, Winooski, VT). Fluorescence of Amplex Red was measured using a 530 nm excitation filter and a 560 nm emission filter.

Total RNA extraction and qRT-PCR

Total cellular RNA was extracted using an RNeasy Mini Kit (Qiagen) and DNase I treatment (Qiagen, Valencia, CA), according to the manufacturer's instructions. Target gene expression was normalized to β-actin rRNA levels, which were assayed by multiplexing with the manufactures 5#VIC-labeled, primer-limited β-actin endogenous control premix. Primers and 5# FAM-labeled Taqman probes were purchased as pre-validated assays and qRT-PCR was performed using an ABI 7900HT (Applied Biosystems, Carlsbad, CA). Relative quantification of target genes was calculated using the 2^{Δ-CT} method. Derivation of the 2^{-ΔCT} equation has been described in Applied Biosystems User Bulletin No. 2 (P/N 4303859).

Circulating inflammatory cytokines:

Interleukin 6 (IL6) and C-reactive protein inflammatory markers were measured via enzyme-linked immunosorbent assay (ELISA) from Alpco (Salem, NH) and R&D Systems (Minneapolis, MN) respectively, according to manufacturer's instructions.

Statistical analysis: Statistics

Results were analyzed with a 2-way ANOVA with a Tukey post-hoc test for multiple comparisons. All data was tested for normality using the Shapiro-Wilk normality test. If it was determined that the data was not normal, a Mann-Whitney test was conducted in place of ANOVA. Results are presented as mean ± SD. The level of significance was set *a priori* at P<0.05.

Results

Fatty acid oxidation

Although there were no significant interactions, there were significant age effects in both red and white skeletal muscle in both wild type and transgenic animals (**Figure 1**). Although CO₂ production was significantly higher in red muscle from 9-month-old mice (**Figure 1A**), ASMs were significantly lower in 6 and 9 month old mice (**Figure 1B**), and total oxidation was significantly lower in 6-month-old mice compared to 3-month-old mice (**Figure 1C**).

In white muscle, CO₂ production was significantly lower in 9-month-old mice compared to 3-month-old mice (**Figure 1D**), ASMs were significantly lower in 6 and 9-month-old mice compared to 3-month-old mice (**Figure 1E**), and total oxidation was significantly lower in 9-month-old mice compared to 3-month-old mice (**Figure 1F**). Additionally, there were trends for an effect of genotype in white skeletal muscle. Post hoc analysis revealed that both CO₂ and total fatty acid oxidation

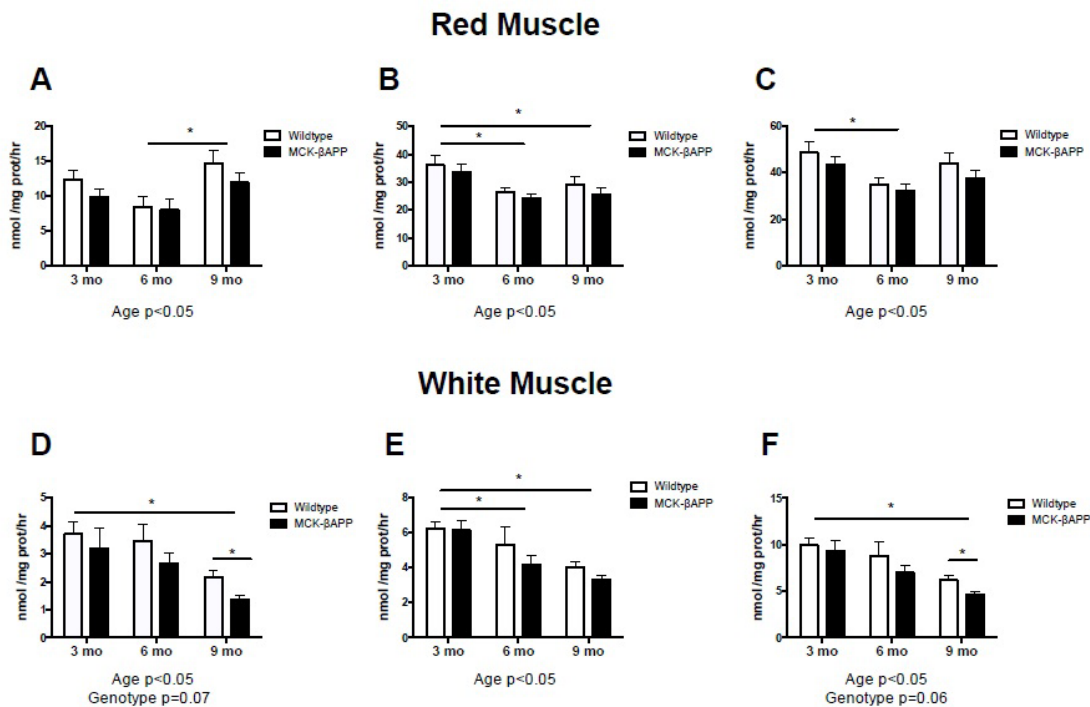


Figure 1 Palmitate oxidation in skeletal muscle from MCK-APP and wild type mice. (A) CO₂ production in red skeletal muscle, (B) Acid soluble metabolite production in red skeletal muscle muscle, (C) Total oxidation in red skeletal muscle, (D) CO₂ production in white skeletal muscle, (E) Acid soluble metabolite production in white skeletal muscle, (F) Total oxidation in white skeletal muscle.

was significantly lower in 9-month-old MCK-APP compared to 9-month-old wild type mice (**Figure 1D** and **Figure 1F**).

Pyruvate dehydrogenase activity (PDH), metabolic flexibility, and oxidative efficiency

There were no significant interactions in pyruvate dehydrogenase activity, metabolic flexibility, or oxidative efficiency in red or white skeletal muscle (**Figure 2**). However, there were age effects.

Pyruvate dehydrogenase activity and metabolic flexibility was significantly higher in red muscle from 9-month-old mice (**Figure 2A** and **2B**) compared to 3-month-old-mice. Additionally, oxidative efficiency was significantly higher in 9-month-old mice compared to both 3 and 6-month-old mice (**Figure 2C**).

In white muscle, pyruvate dehydrogenase activity was significantly higher in 6-month-old mice compared to 3-month-old mice (**Figure 2D**). However, oxidative efficiency was significantly lower in 9-month-old mice compared to 6-month-old mice (**Figure 2F**). Additionally, there was a trend for an effect of genotype in white skeletal muscle. There was a trend for reduced metabolic flexibility in 6 and 9-month-old -MCK-APP mice compared to wild type mice (**Figure 2E**). Additionally, 9-month-old-MCK-APP exhibited reduced oxidative efficiency compared to wild type mice (**Figure 2F**).

Metabolic enzyme activity

Metabolic enzymatic activity is displayed in **Figure 3**. While there were no significant interactions or genotype effects with regards to Citrate Synthase (CS), β -hydroxyacyl-CoA dehydrogenase (β -HAD) and Malate Dehydrogenase (MDH) activity in red or

white skeletal muscle, there were age effects.

In red muscle, citrate synthase was significantly lower in 6-month-old animals compared to both 3 and 9 month old mice (**Figure 3A**), β -HAD was significantly higher in 9 month old mice (**Figure 3B**) compared to 3 and 6 month-old-mice, and MDH was significantly lower in 6-month-old mice compared to both 3 and 9-month-old mice (**Figure 3C**). There was no effect of genotype with regards to enzyme activity in red skeletal muscle. There were also no significant age or genotype differences observed in white skeletal muscle (**Figure 3D-3F**).

Respiration in isolated mitochondria

Mitochondrial oxygen consumption was assessed in red skeletal muscle only and is displayed in **Figure 4**. There were no significant interactions with any of the measures of mitochondrial oxygen consumption, however there were significant age effects. RCR and state three respiration was significantly lower in 9-month-old mice compared to 3 and 6-month-old mice (**Figure 4A** and **4C**). State 2 respiration and state 3u respiration was significantly lower in 9-month-old mice compared to 6-month-old mice (**Figure 4B** and **4E**). There were no significant differences in state 4_o respiration (**Figure 4D**).

Reactive oxygen species generation

There were no significant differences in ROS generation between transgenic and wild type animals at any of the time points measured (**Figure 5**). There was, however, significant differences in ROS production from complex I (**Figure 5A**) and complex III (**Figure 5B**), between 6 and 9-month-old mice (**Figure 5C**).

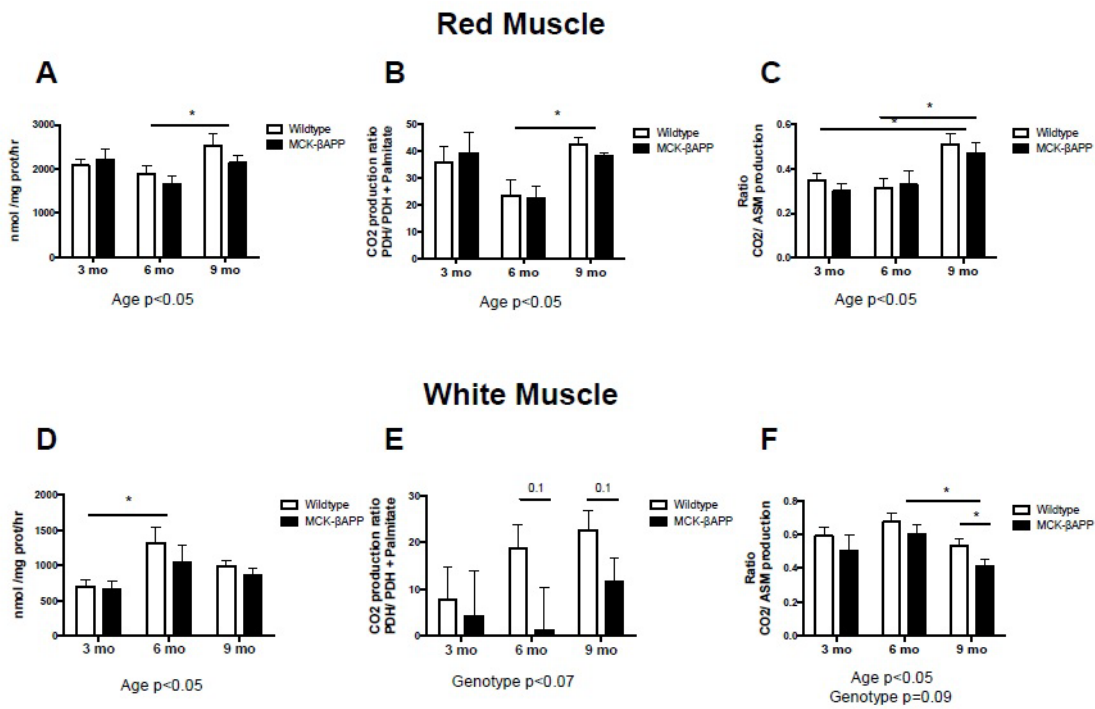


Figure 2 Pyruvate dehydrogenase activity, metabolic flexibility, and oxidative efficiency in skeletal muscle from MCK-APP and wild type mice. (A) Pyruvate oxidation in red skeletal muscle, (B) Metabolic flexibility in red skeletal muscle, (C) Oxidative efficiency in red skeletal muscle, (D) Pyruvate oxidation in white skeletal muscle, (E) Metabolic flexibility in white skeletal muscle, (F) Oxidative efficiency in white skeletal muscle.

mRNA content in red and white skeletal muscle from MCK β -APP mice and their littermate controls

mRNA content for markers of autophagy was assessed in red and white skeletal muscle (Figure 6). LC3 mRNA was significantly higher in red muscle of 3 and 9-month-old MCK β -APP mice compared to wild type mice (Figure 6A). Beclin mRNA was significantly higher in red and white muscle from MCK β -APP 3-month and 9-month-old MCK β -APP mice compared to wild type mice (Figure 6B-6D).

Markers of systemic inflammation in MCK-APP mice and wild-type littermates

To assess systemic inflammation, fasting measures of C-reactive protein (CRP) and interleukin-6 (IL-6) were measured and are displayed in Figure 7. Although, at 3-months CRP concentrations were slightly lower in MCK-APP mice compared to wild type animals (p=0.08), there were no significant differences between genotype observed at 6 or 9-months (Figure 7A). Serum IL-6 measurements showed no significant differences between MCK-APP and wild-type mice at any time points (Figure 7B).

Discussion

sIBM is the most prevalent muscle disease among the elderly and risk increases with age [1]. There is no known cause or successful treatment for the disorder leaving patients with limited options following diagnosis [3]. The current study tested whether mitochondrial dysfunction is present in skeletal muscle in a mouse model of sIBM. Contrary to our hypothesis, the results demonstrate that mitochondrial function is not disrupted in MCK-

APP mice. Additionally, there were no differences in substrate metabolism or reactive oxygen species generation in red muscle from MCK-APP mice compare to the wild types. Conversely, decreased fat metabolism and decreased oxidative efficiency in white muscles from MCK-APP mice compared to wild type mice was observed in the current study. Increased mRNA content of LC3, a marker of autophagy, was also reported in MCK-APP mice compared to wild type controls.

These results are in contrast to data reported by Boncompagni et al. [8] which demonstrated structural and functional alterations in mitochondria of 2-3 month old MCK-APP mice. Their study reported disruption of TCA cycle activity, i.e., reductions in radiolabeled glutamate, and succinate, in MCK-APP mice compared to wild type controls. Increased ROS production in MCK-APP mice was also reported in this study. Differences in findings between the current study and Boncompagni may be due to the differences in methodologies used to assess mitochondrial function. While the current study assessed mitochondrial function by measuring mitochondrial oxygen consumption, fatty acid oxidation, and oxidative enzyme activity, Boncompagni's study assessed structural and morphological differences within the muscle along with TCA cycle activity (rate of appearance and disappearance of radiolabeled glutamate and succinate) and membrane potential. Furthermore, the two studies used different techniques to assess reactive oxygen species production. The precise measurement of ROS in cells and tissues is challenging because of extremely low concentrations and short lifespan. The current study employed Amplex Red to assess H₂O₂ as a marker of ROS production. Amplex red is highly specific and sensitive, with

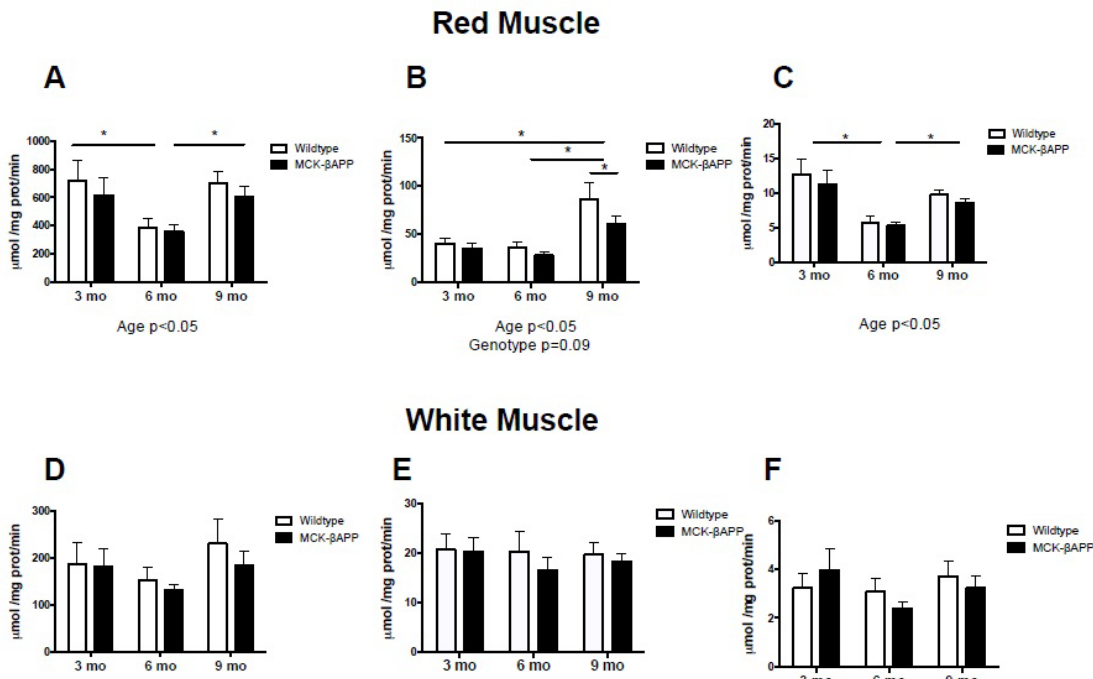


Figure 3 Enzyme activity in skeletal muscle from MCK-APP and wild type mice. (A) Citrate synthase activity in red skeletal muscle, (B) β-hydroxyacyl-CoA dehydrogenase activity in red skeletal muscle, (C) Malate dehydrogenase activity in red skeletal muscle, (D) Citrate synthase activity in white skeletal muscle, (E) β-hydroxyacyl-CoA dehydrogenase activity in white skeletal muscle, (F) Malate dehydrogenase activity in white skeletal muscle.

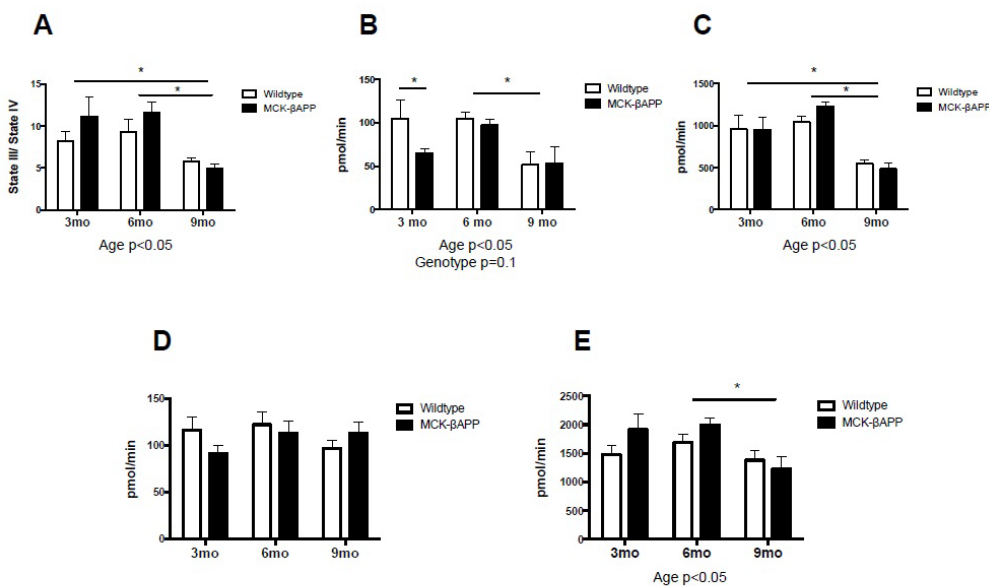


Figure 4 Mitochondrial bioenergetics in isolated mitochondria from red skeletal muscle from MCK-APP and wild type mice. (A) Respiratory control ratio, (B) State 2 respiration rate, (C) State 3 (ADP stimulated) respiration rate, (D) state 4o (oligomycin insensitive) respiration rate, and (E) state 3u (FCCP-stimulated) respiration rate.

a limit of detection of ≈ 5 pmol of H_2O_2 . Also, the stoichiometry of Amplex Red and H_2O_2 is 1:1; thus, the assay results are linear over the range of values encountered in tissues and cells [22]. On the other hand, Boncompagni assessed ROS production by measuring intracellular ROS concentrations using 5- (and 6) chloromethyl-2',7'-dichlorodihydrofluorescein diacetate (DCFH-DA). The DCFH-DA technique is often criticized since photoreduction of DCF

results in artificial production of a semiquinone radical that in turn can reduce oxygen to free radicals, and the oxidation of DCFH to the DCF can be self-catalyzed by peroxidases [23]. Therefore, conditions that alter cellular peroxidase levels could affect DCF fluorescence independent of actual cellular ROS levels [23,24].

There were also differences between the two studies with regards to the fiber types assessed. While Boncompagni

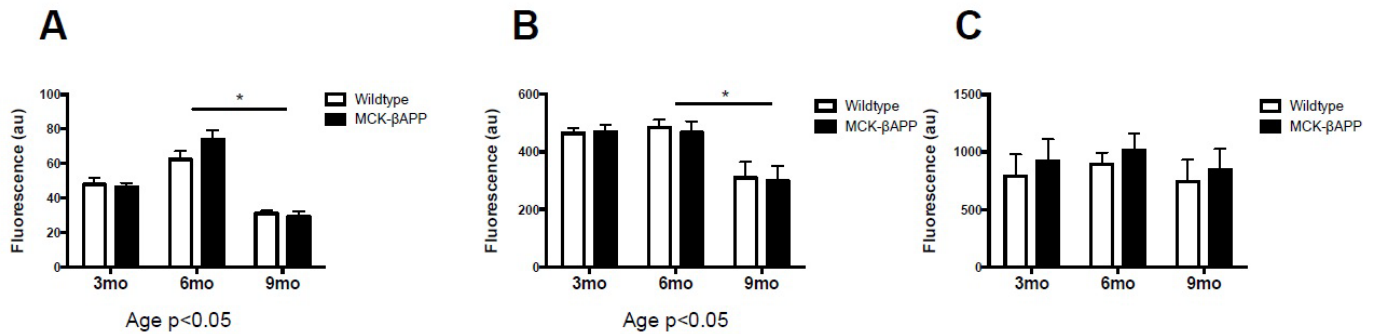
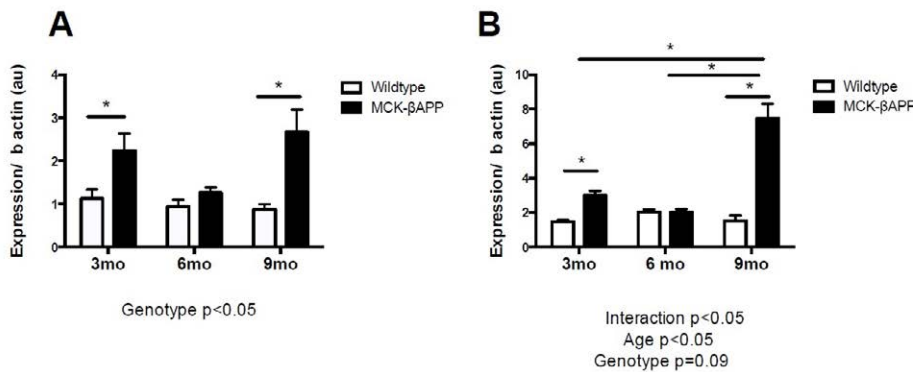


Figure 5 Reactive oxygen species (ROS) production in isolated mitochondria from red skeletal muscle from MCK-APP and wild type mice. (A) ROS production from complex one, (B) ROS production from complex three, (C) ROS production from reverse electron transport.

Red Muscle



White Muscle

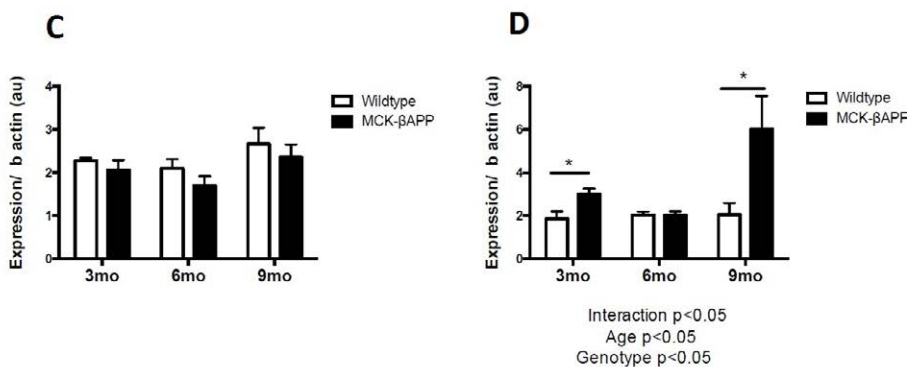


Figure 6 Gene expression of autophagy markers in red and white skeletal muscle from MCK-APP and wild type mice. (A) LC3 expression in red skeletal muscle, (B) Beclin expression in red skeletal muscle, (C) LC3 expression in white skeletal muscle, (D) Beclin expression in red skeletal muscle.

et al. [8] examined mitochondrial parameters in extensor digitorum longus (EDL) and flexor digitorum brevis (FDB), both predominately white muscle types, the current study assessed quadriceps and gastrocnemius muscles, both considered mixed muscle groups. We chose these muscle groups because they are more physiologically relevant to the muscles affected in patients

diagnosed with sIBM (vastus lateralis) [25]. It is important to note that red and white muscle was separated for the current studies and while we did not measure mitochondria bioenergetics from white skeletal muscle we did note a decrease in fat oxidation (total oxidation and CO₂ production) and oxidative efficiency in white gastrocnemius and quadriceps femoris muscle. These

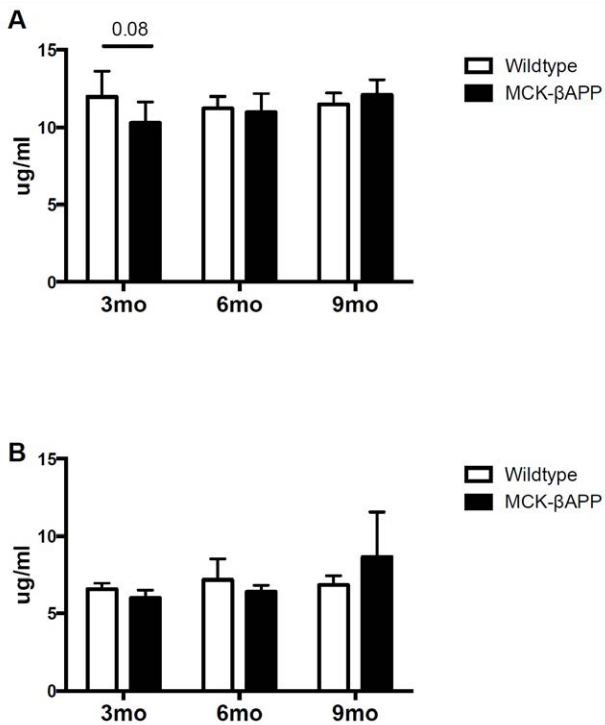


Figure 7 Fasting, circulating inflammatory markers from MCK-APP and wild type mice. (A) C-reactive protein concentration, (B) Interleukin-6 concentration.

results also coincide with the previous human proteomic studies that found reductions in proteins exclusively in the white muscles [26]. Finally, Boncompagni et al. [8] identified and separated “amyloid beta affected” muscle fibers for their study. These fibers were characterized by amyloid beta accumulation, amorphous material, the presence of vacuoles, and mitochondrial structural alterations. Not all muscle fibers within a muscle are affected by sIBM and in fact affected fibers are interspersed between many healthy fibers [8]. It was not possible in the current study to only select affected fibers. As a result, the lack of differences between MCK-APP and wild type mice observed in the current study could be due to dilution of affected fibers interspersed within many healthy fibers. Nonetheless, these data along with the work from Boncompagni et al. [8] suggest that other factors such as amyloid beta accumulation may be required for the initiation of mitochondrial abnormalities in skeletal muscle and are therefore more likely the cause (or causes) of sIBM.

While data from the current study do not indicate mitochondria as a primary factor in the initial development of sIBM, it is possible that mitochondria may still be a contributor to disease

progression. The current study specifically chose to employ 3, 6 and 9-month old MCK-APP mice to explore the effects of mitochondrial dysfunction prior to the occurrence of sIBM symptoms including inflammation, amyloid beta accumulation, and motor defects [27,28]. It is possible that mitochondrial dysfunction occurs following disease onset and may contribute to the decreased functionality occurring with disease progression. This idea is supported by previous work conducted in humans, in which mitochondrial abnormalities are observed following diagnosis [29-31].

Data from the current study demonstrate increase in LC3 mRNA in MCK-APP mice, which is an indication of increased autophagosome formation. During autophagy, LC3 is lipidated, and the LC3-phospholipid conjugate (LC3-II) is localized to the autophagosome [32]. The autophagosome travels through the cytoplasm of the cell to a lysosome, which then fuses with the autophagosome resulting in the formation of the autolysosome. As such, the LC3-phospholipid conjugate system is important for the development and transport of the autophagosome [33]. Additionally, any disruption in any of the steps of autophagy, i.e., disruption in lysosome formation or fusion of the autophagosome with the lysosome, could result in the accumulation of damaged cellular debris including degraded cellular protein. While the current study suggests an increase in autophagosome formation, it is not evident whether this results in the formation of the autolysosome or if there are defects in the formation of the lysosome or autolysosome.

There are some limitations to the current work. For example, while the MCK-APP animal model is an accepted animal model for the study of sIBM, the role of amyloid beta precursor protein and subsequent accumulation of amyloid beta protein in the development of the disease is still up for debate. In addition, in order to understand the effects of age on the role of the mitochondria in the development of sIBM, additional time points with older animals (12, 15, 18 months) should be investigated. sIBM is an age-related disease and the effect of age is an important factor to be investigated in MCK-APP animals.

Summary

The present work demonstrates that mitochondrial abnormalities and ROS production are not observed in red gastrocnemius and quadriceps femoris muscle and therefore do not appear to be a primary cause of sIBM like symptoms in MCK-APP mice. Nonetheless, there is a significant reduction in fat metabolism as well as an up regulation of autophagic pathways suggesting that certain alterations in skeletal muscle from MCK-APP mice occur prior to the onset of classic disease symptoms.

References

- Machado P, Miller A, Holton J, Hanna M (2009) Sporadic inclusion body myositis: an unsolved mystery. *Acta Reumatol Port* 34: 161-182.
- Garlepp MJ, Mastaglia FL (1996) Inclusion body myositis. *J Neurol Neurosurg Psychiatry* 60: 251-255.
- Askanas V, Engel WK (2008) Inclusion-body myositis: muscle-fiber molecular pathology and possible pathogenic significance of its similarity to Alzheimer's and Parkinson's disease brains. *Acta Neuropathol* 116: 583-595.
- Chou SM (1993) Inclusion body myositis. *Baillieres Clin Neurol* 2: 557-577.
- Mastaglia FL, Laing BA, Zilko P (1993) Treatment of inflammatory myopathies. *Baillieres Clin Neurol* 2: 717-740.
- Kitazawa M, Green KN, Caccamo A, LaFerla FM (2006) Genetically augmenting A β 42 levels in skeletal muscle exacerbates inclusion body myositis-like pathology and motor deficits in transgenic mice. *The American journal of pathology* 168: 1986-1997.
- Shtifman A, Ward CW, Laver DR, Bannister ML, Lopez JR, et al. (2010) Amyloid- β protein impairs Ca $^{2+}$ release and contractility in skeletal muscle. *Neurobiol Aging* 31: 2080-2090.
- Boncompagni S, Moussa CE, Levy E, Pezone MJ, Lopez JR, et al. (2012) Mitochondrial dysfunction in skeletal muscle of amyloid precursor protein-overexpressing mice. *J Biol Chem* 287: 20534-20544.
- Rhein V (2009) Amyloid-beta and tau synergistically impair the oxidative phosphorylation system in triple transgenic Alzheimer's disease mice. *Proceedings of the National Academy of Sciences of the United States of America* 106: 20057-20062.
- Sugarman MC, Yamasaki TR, Oddo S, Echegoyen JC, Murphy MP, et al. (2002) Inclusion body myositis-like phenotype induced by transgenic overexpression of beta APP in skeletal muscle. *Proc Natl Acad Sci U S A* 99: 6334-6339.
- Vattemi G, Engel WK, McFerrin J, Askanas V (2003) Cystatin C colocalizes with amyloid-beta and coimmunoprecipitates with amyloid-beta precursor protein in sporadic inclusion-body myositis muscles. *J Neurochem* 85: 1539-1546.
- Fukuchi K, Pham D, Hart M, Li L, Lindsey JR (1998) Amyloid-beta deposition in skeletal muscle of transgenic mice: possible model of inclusion body myopathy. *Am J Pathol* 153: 1687-1693.
- Jin LW, Hearn MG, Ogburn CE, Dang N, Nochlin D, et al. (1998) Transgenic mice over-expressing the C-99 fragment of betaPP with an alpha-secretase site mutation develop a myopathy similar to human inclusion body myositis. *Am J Pathol* 153: 1679-1686.
- Luo YB, Johnsen RD, Griffiths L, Needham M, Fabian VA, et al. (2013) Primary over-expression of A β PP in muscle does not lead to the development of inclusion body myositis in a new lineage of the MCK-A β PP transgenic mouse. *Int J Exp Pathol* 94: 418-425.
- Gao S, McMillan RP, Jacas J, Zhu Q, Li X, et al. (2014) Regulation of substrate oxidation preferences in muscle by the peptide hormone adropin. *Diabetes* 63: 3242-3252.
- Zhang S (2014) Chickens from lines selected for high and low body weight show differences in fatty acid oxidation efficiency and metabolic flexibility in skeletal muscle and white adipose tissue. *International journal of obesity* 38: 1374-1382.
- Anderson AS, Roberts PC, Frisard MI, McMillan RP, Brown TJ, et al. (2013) Metabolic changes during ovarian cancer progression as targets for sphingosine treatment. *Exp Cell Res* 319: 1431-1442.
- Power RA, Hulver MW, Zhang JY, Dubois J, Marchand RM, et al. (2007) Carnitine revisited: potential use as adjunctive treatment in diabetes. *Diabetologia* 50: 824-832.
- Frezza C, Cipolat S, Scorrano L (2007) Organelle isolation: functional mitochondria from mouse liver, muscle and cultured fibroblasts. *Nat Protoc* 2: 287-295.
- Quinlan CL, Gerencser AA, Treberg JR, Brand MD (2011) The mechanism of superoxide production by the antimycin-inhibited mitochondrial Q-cycle. *J Biol Chem* 286: 31361-31372.
- Quinlan CL, Treberg JR, Perevoshchikova IV, Orr AL, Brand MD (2012) Native rates of superoxide production from multiple sites in isolated mitochondria measured using endogenous reporters. *Free radical biology & medicine* 5: 1807-1817.
- Dikalov S, Griendling KK, Harrison DG (2007) Measurement of reactive oxygen species in cardiovascular studies. *Hypertension* 49: 717-727.
- Rota C, Chignell CF, Mason RP (1999) Evidence for free radical formation during the oxidation of 2'-7'-dichlorofluorescein to the fluorescent dye 2'-7'-dichlorofluorescein by horseradish peroxidase: possible implications for oxidative stress measurements. *Free radical biology & medicine* 27: 873-881.
- Rota C, Fann YC, Mason RP (1999) Phenoxy free radical formation during the oxidation of the fluorescent dye 2',7'-dichlorofluorescein by horseradish peroxidase. Possible consequences for oxidative stress measurements. *The Journal of biological chemistry* 27: 28161-28168.
- Kobayashi YM, Rader EP, Crawford RW, Campbell KP (2012) Endpoint measures in the mdx mouse relevant for muscular dystrophy pre-clinical studies. *Neuromuscul Disord* 22: 34-42.
- Parker KC, Kong SW, Walsh RJ, Bch, Salajegheh M, Moghadaszadeh B, et al. (2009) Fast-twitch sarcomeric and glycolytic enzyme protein loss in inclusion body myositis. *Muscle Nerve* 39: 739-753.
- Askanas V, Engel WK, Alvarez RB (1992) Light and electron microscopic localization of beta-amyloid protein in muscle biopsies of patients with inclusion-body myositis. *Am J Pathol* 141: 31-36.
- Schmidt J (2008) Interrelation of inflammation and APP in sIBM: IL-1 beta induces accumulation of beta-amyloid in skeletal muscle. *Brain : a journal of neurology* 1 1228-1240.
- Askanas V, Alvarez RB, Engel WK (1993) beta-Amyloid precursor epitopes in muscle fibers of inclusion body myositis. *Ann Neurol* 34: 551-560.
- Askanas V, McFerrin J, Alvarez RB, Baqué S, Engel WK (1997) Beta APP gene transfer into cultured human muscle induces inclusion-body myositis aspects. *Neuroreport* 8: 2155-2158.
- Askanas V (1996) Transfer of beta-amyloid precursor protein gene using adenovirus vector causes mitochondrial abnormalities in cultured normal human muscle. *Proceedings of the National Academy of Sciences of the United States of America* 9 1314-1319.
- Tanida I, Minematsu-Ikeguchi N, Ueno T, Kominami E (2005) Lysosomal turnover, but not a cellular level, of endogenous LC3 is a marker for autophagy. *Autophagy* 1: 84-91.
- Jessup W, Bodmer JL, Dean RT, Greenaway VA, Leoni P (1984) Intracellular turnover and secretion of lysosomal enzymes. *Biochemical Society transactions* 1: 529-531.